

1
2
3
4
5
6
7
8
9
10
11
12
13
14
15
16
17
18
19
20

Assessment of Land Use and Land Cover Dynamics in the Cavally River Watershed, Western Côte d'Ivoire

ABSTRACT

This study aims to evaluate the spatiotemporal dynamics of land use and land cover within a sub-watershed of the Cavally River. To achieve this objective, four Landsat satellite images were acquired from the U.S. Geological Survey website. The dataset includes Landsat Thematic Mapper (TM5) imagery from 1985, Landsat Enhanced Thematic Mapper Plus (ETM+) imagery from 2000, and Landsat 8–9 Operational Land Imager (OLI) imagery from 2015 and 2025.

The methodological approach relied on the application of remote sensing techniques. Image preprocessing and processing workflows enabled the production of land-cover maps for each reference year. Five major land-cover classes were identified from the Landsat images: dense vegetation, degraded vegetation, agricultural areas, settlements and bare soils, and water bodies.

Area estimates derived from the classification results show a substantial decline in dense vegetation, decreasing from 226.49 km² (48.74%) in 1985 to 40.96 km² (8.81%) in 2025. This pronounced loss of forest cover is largely attributable to mining activities and rapid population growth, which have intensified anthropogenic pressures on the environment. Concurrently, agricultural land expanded considerably, from 39.79 km² (8.56%) in 1985 to 116.19 km² (25%) of the total area of the sub-watershed in 2025, reflecting increasing demand for arable land.

Keywords: Dynamics, Land Use, Watershed, Cavally River

21
22

23
24
25
26
27
28
29
30

31
32 **1. INTRODUCTION**

33 Rapid global population growth is placing intense pressure on the land resources needed to support livelihoods,
34 leading to widespread conversion of natural landscapes and environmental disruption, particularly deforestation
35 (Tong and Qiu, 2020). Forests are among the most productive terrestrial ecosystems in the world. They are
36 essential to life on Earth and to sustainable development (FAO, 2018). It is worth noting, unfortunately, that this
37 resource is declining worldwide, and particularly in Africa. Between 2010 and 2020, this continent recorded the
38 highest annual rate of net forest loss, at 3.9 million hectares (FAO, 2020). This deforestation or conversion of
39 forest to other land uses (FAO, 2020) has become a major concern, both locally and globally. It has a significant
40 impact on biodiversity and several ecosystem services (Biaou et al., 2019). For watersheds, forests have a
41 beneficial influence on the flow and yield of springs, on soil protection, and on rainfall (Andréassian, 2004). The
42 ideal would therefore be to maintain or increase them.

43 Furthermore, Africa is a continent with significant mining potential, holding 30% of the world's reserves of
44 minerals critical to the global economy and nearly 40% of the world's gold (Amedee, 2017). In Côte d'Ivoire, the
45 sharp decline in agricultural commodity prices between 1980 and 1990, combined with major discoveries of
46 mineral deposits, enabled the Ivorian government to revitalize the mining sector and consider making the
47 extractive industry the second pillar of its economy (Soro, 2011). This sector contributed 2.3% to GDP (including
48 0.7% from gold) in 2012 and employs approximately 30,000 people (DGMG, 2013).

49 The subprefecture of Zouan-Hounien, with its significant mining potential, is part of this production drive. Indeed,
50 the Ity mining area, located near the Cavally River in western Côte d'Ivoire, specifically in the Zouan-Hounien
51 department, is home to an industrial mining operation (SMI) as well as several artisanal gold mining sites
52 surrounding it. Once dominated by agriculture, this area is now characterized by intense gold mining activities
53 that attract a significant portion of the population (men, women, and children), particularly young people.
54 However, population growth and the rapid expansion of mining activities in the Cavally River watershed have
55 led to profound changes in vegetation cover and land use. These changes are characterized by significant spatial
56 expansion, often poorly managed.

57 The objective of this study is to assess the dynamics of land use and vegetation cover in order to promote better
58 environmental management in the Cavally River basin, using GIS and remote sensing tools.

59
60
61 **2. MATERIAL AND METHODS**

62
63
64 **2.1 Presentation of the Study Area**

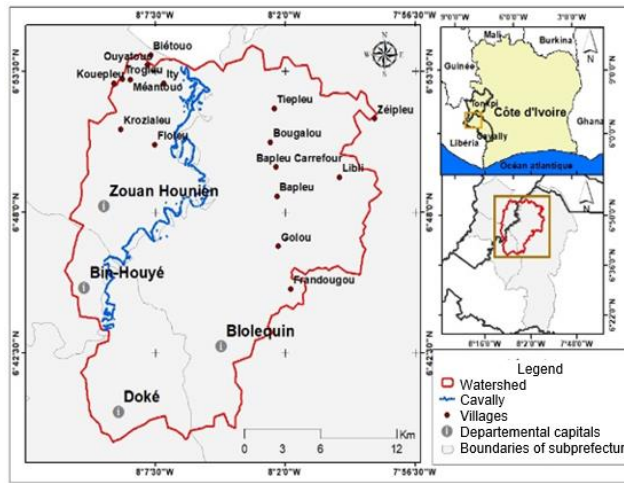
65
66
67 The Cavally River watershed is shared by Côte d'Ivoire, Guinea, and Liberia. It is a transboundary basin located between
68 longitudes 8°4' and 7°7' West and latitudes 6°8' and 7°9' North. The Cavally River forms a natural boundary between Côte
69 d'Ivoire and Liberia along its middle and lower reaches. It originates in Guinea, north of Mount Nimba, at an altitude of 600
70 m, and stretches over a length of 700 km.

71 The sub-watershed examined in this study, whose outlet is located in Bin-Houyé in the Zouan-Hounien department, covers
72 an area of approximately 464.37 km² (Figure 1).
73

74
75 **2.1.1 Geological Context**
76

77 Prospecting work carried out between 1962 and 1968 by SODEMI revealed strong gold mineralization in the Ity area, where
78 intense artisanal gold mining activities had already existed during the 1940s and 1950s (Papon, 1973). The dominant

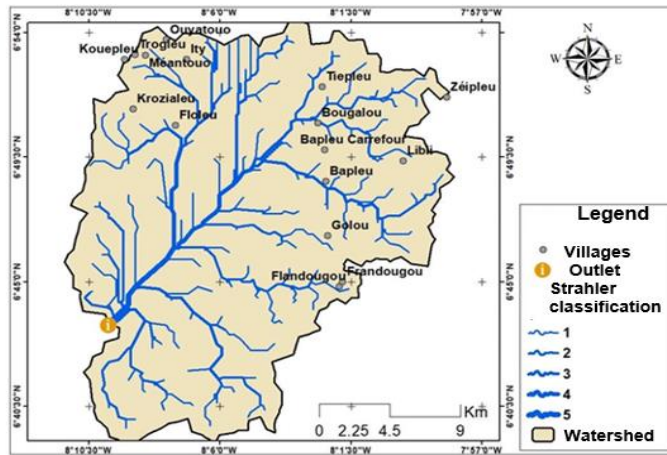
79 geological component belongs to the Ity sequence, characterized by metabasalts within a fine-grained and carbonated
 80 environment near the base, giving rise to a sedimentary sequence with varying amounts of carbonate horizons.
 81 This sequence is intruded by mafic bodies (gabbros and granodiorites resulting from two distinct magmatic events) that are
 82 in contact with the metamorphosed carbonate rocks, which show a spatial relationship with the mineralization. Skarn and
 83 hornfels facies are generally associated with nearby carbonate rocks in contact with the granodiorite body in the Flotou
 84 area (Feybesse et al., 1990; Brou, 2019).
 85



86
 87 Figure 1: Location Map of the Study Area
 88
 89

90 **2.1.2 Hydrography of the Study Area**
 91

92 The Cavally River and its main tributary, the Nuon, drain the entire Montagnes Region (Ettien, 2005). The Cavally watershed,
 93 from which the 700 km long river takes its name, is characterized by a hydrographic network composed of numerous small
 94 streams, the most important of which are the Nilpi, Doui, Zo, and Klo (Tricart et al., 1973). At its source, the Cavally is known
 95 as the Djougou, and it receives the Dire River on its left bank. Up to Toulépleu, it is fed only by very small tributaries.
 96 The sub-watershed examined in this study, whose outlet is located south of Floué in the locality of Zouan-Hounièn, covers
 97 an area of approximately 471.37 km².
 98
 99



100
 101
 102
 103
 104
 105
 106
 107
 108
 109
 110
 111
 112
 113
 114
 115 Figure 2 : Map of the Hydrographic Network of the Study Area
 116

117 **2.2 Material**

118 The materials consist of satellite image data and computer equipment.

119 **Satellite Image Data**
 120

To better understand land-use dynamics, four Landsat satellite images were downloaded from the U.S. website <https://www.earthexplorer.gov/>. These include Landsat Thematic Mapper (TM5) images from 1985, Landsat Enhanced Thematic Mapper (ETM+) images from 2000, and Landsat 8–9 Operational Land Imager images from 2015 and 2025. The images acquired at different dates were used to produce land-use maps for the years 1985, 2000, 2015, and 2025.

2.3 Methods

2.3.1 Mapping of Land Use Dynamics

The methodology adopted for mapping land-use dynamics is as follows:

• Band Stacking

Band stacking in ArcGIS consists of combining the individual bands of a Landsat image. Indeed, downloading Landsat satellite images provides an output file in a zipped folder containing several bands (B1, B2, B3...B12). Before processing the images, these bands must be merged to produce a single multiband image (Derdjini H., 2017).

• Landsat Image Preprocessing

Landsat image preprocessing is a crucial step in satellite image analysis. Its purpose is to correct variations in data distribution caused by temporal differences in image acquisition and to extract the study area. These variations are mainly due to factors such as solar elevation angle, Earth–sun distance, atmospheric conditions, sensor calibration, and viewing geometry, all of which affect pixel digital values (Carine et al., 2023).

Two types of corrections were applied during preprocessing:

- atmospheric corrections
- radiometric corrections

• Landsat Image Processing

Image processing involves the use of vegetation indices and color composites to separate information such as vegetation, settlements, water bodies, and forest cover.

➤ Vegetation Index

The vegetation index, also known as the Normalized Difference Vegetation Index (NDVI), is a tool used in remote sensing to assess vegetation density in a given area. This index is calculated from land-surface reflectance measurements in the near-infrared and red portions of the electromagnetic spectrum. It allows vegetation to be distinguished from other land-cover types. The equation is written as:

$$NDVI = \frac{(PIR - R)}{(PIR + R)}$$

➤ Color composite

Color composite techniques allow clearer and more visually appealing representations of satellite images. Spectral band combinations (5,4,3) and (4,3,2) were used to generate the color composites of the downloaded images. The principle is to combine three spectral bands to produce a color-rich composite image.

• Classification and Validation of the Land-Cover Map

➤ Supervised Classification

According to several authors (Pontius, 2000; Yao, 2009), there are two major types of image classification: supervised and unsupervised classification. This study focuses on supervised classification. This method consists of assigning pixels to the closest training samples based on a Bayesian distance, which evaluates the probability that a pixel belongs to a given class (Aka, 2014).

In this study, the maximum likelihood classification method was chosen. This algorithm is widely used in supervised classification and is considered the most effective for producing thematic maps in land-use and land-cover studies (Kouassi, 2007).

2.3.2 Validation of the Supervised Classification and Field Survey

176
177
178
179
180
181
182
183
184
185
186
187
188
189
190
191
192
193
194
195
196
197
198
199
200
201
202
203
204
205

To better assess the accuracy of the different land-use/land-cover maps, the Kappa index and the confusion matrix will be used. The Kappa index evaluates, within the confusion matrix, the level of agreement between the classification results and the ground-truth data.

3. RESULTS AND DISCUSSION

3.1 Analysis of the spatiotemporal dynamics of land use and land cover

3.1.1 Discrimination of Land Use Types Using Color Composites

The spectral bands 5, 4, 3 and 4, 3, 2 were used to generate color composites for better discrimination of the different land-use and land-cover types. This resulted in various color combinations that allowed a clearer distinction of land-cover categories. Thus, five (05) land-use classes were identified from the 1985 Landsat TM images, the 2000 ETM+ images, and the 2015 and 2025 OLI images. These classes are: dense vegetation, degraded vegetation (cleared forest and fallow), agricultural areas (perennial crops and food crops), settlements, bare soils, and water bodies.

3.1.2 Observation of Land-Use Classes in the Study Area

In the Cavally sub-watershed, dense forest corresponds to areas of very high vegetation cover. Degraded forest consists of patches of cleared forest, fallow land (both old and young), and forest remnants covering cultivated areas. Bare soils and settlements include village settlements, areas stripped of vegetation due to artisanal gold mining activities, and industrial mining operations (SMI). Agricultural areas include cash crops (coffee, cocoa, rubber, etc.) as well as food crops (maize, cassava, plantain, etc.), as illustrated in the map. The water class represents the hydrographic network of the area, composed of the Cavally River and its various tributaries. It also includes all water reservoirs created by artisanal mining activities and by the SMI.



206
207
208
209
210

Plate: Agricultural Area Class (Cassava cultivation on an old mining site (A), maize cultivation (B), cashew plantation (C), rubber plantation (D))



Photo 1: Inhabited Area Class (A) and Bare Soil (eroded soil) (B)



Photo 2: Class of Selected Types of Degraded Vegetation in the Study Area



Photo 3: Water Class (the Cavally River during low-flow period)

3.2 Evaluation of the Supervised Classification and Mapping of Land Use and Land Cover in the Study Area (1985 – 2000 – 2015 – 2025)

3.2.1 Analysis of the Confusion Matrices for the 1985 – 2000 – 2015 – 2025 Images

The results obtained after classifying the satellite images generated different confusion matrices. These matrices show the number of correctly classified pixels located on the diagonal and the number of misclassified pixels located off the diagonal.

◆ The confusion matrix from 1985 gives an overall accuracy of 65% and a kappa coefficient of 0.55. The highest level of confusion is 4, located between degraded and dense vegetation.

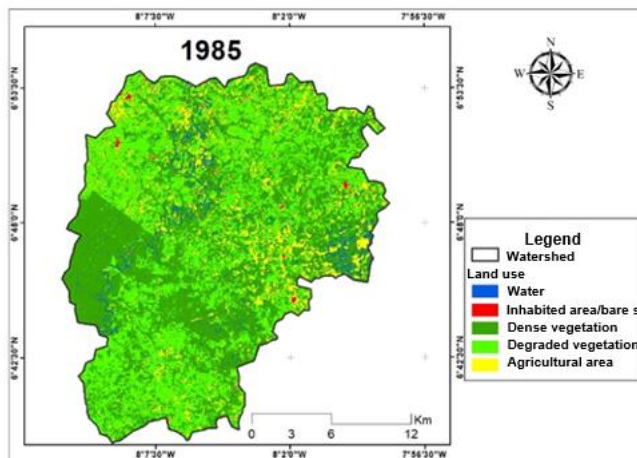
◆ The confusion matrix from 2000 gives an overall accuracy of 72% and a kappa coefficient of 0.63. The highest level of confusion is 4, located between degraded and dense vegetation.

234 ♦ The confusion matrix from 2015 gives an overall accuracy of 78% and a kappa coefficient of 0.71. The highest level of
235 confusion is 5, located between degraded and dense vegetation.

236 ♦ The confusion matrix from the year 2025 gives an overall accuracy of 87% and a kappa coefficient of 0.8. The greatest
237 confusion is 3 and is located between degraded vegetation and dense vegetation.

238 **3.2.2 Presentation of land cover maps and calculation of image areas**

239 The processing and preprocessing performed on the Landsat images allowed for the creation of various land cover maps.
240 The figures and tables below present the different results obtained after image processing. Figure 3 shows the land cover
241 map for the period 1985.



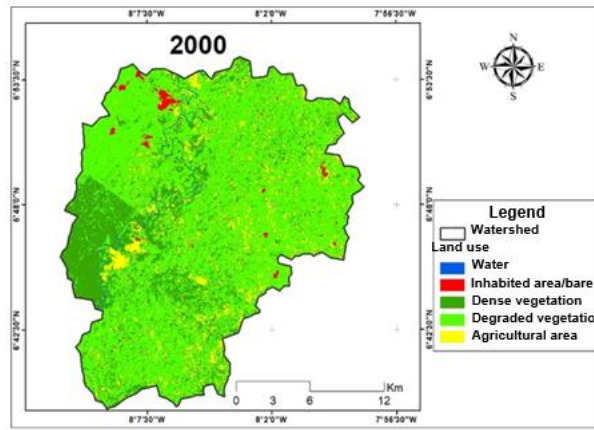
242
243 Figure 3: Land use map for the year 1985

244 The land cover map for 1985 shows that dense vegetation and degraded vegetation cover a significant proportion of the
245 land, while areas classified as inhabited/bare soil and agricultural land are small. Table 1 shows the different surface areas
246 of the land cover units.

247 **Table 1. Image Area 1985**

Classes	Areas in Km ²	Percentages (%)
Water	12.24	2.63
Inhabited area and bare soil	3.67	0.78
Dense vegetation	226.49	48.74
Degraded vegetation	182.43	39.26
Agricultural area	39.79	8.56

248
249
250 ♦ The year 2000 shows a change in the classes of degraded vegetation, agricultural area, inhabited area, and bare soil,
251 and a decrease in dense vegetation and water. The land cover map for the year 2000 is illustrated in Figure 4.



252
253 Figure 4: Land cover map for the year 2000

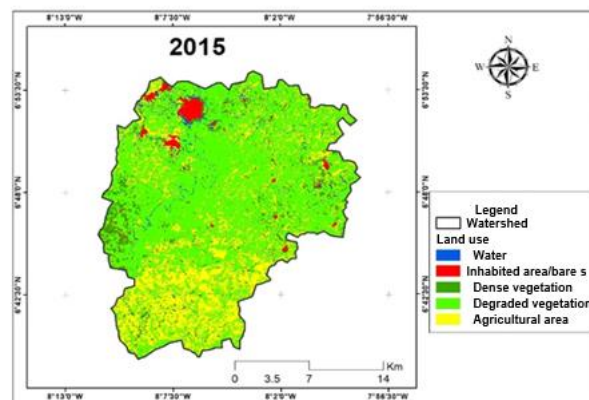
254 Table 2 shows the evolution of the areas, which varies according to the land cover units. The larger areas are those of the
255 degraded vegetation and dense vegetation classes.

256 **Table 2. Image Area 2000**

Classes	Areas in Km ²	Percentages (%)
Water	2	0.43
Inhabited area and bare soil	3.87	0.83
Dense vegetation	109.34	23.57
Degraded vegetation	305.56	65.88
Agricultural area	42.98	9.26

257
258

259 ♦ The year 2015 shows a gradual evolution of the classes habitat/bare soil, agricultural area and water and a reduction of
260 the classes degraded vegetation and dense vegetation. Figure 5 presents the land cover map for the year 2015.



261
262 Figure 5: Land cover map for the year 2015

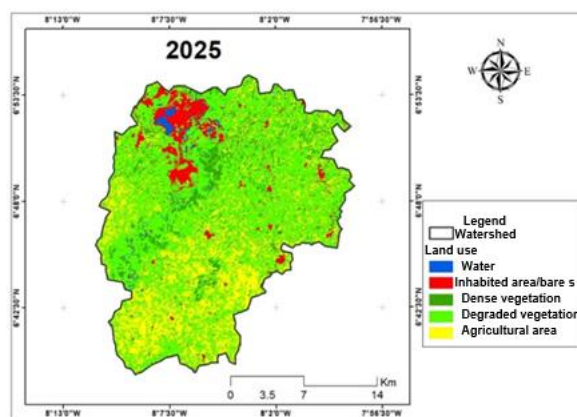
263 Table 3 shows the evolution of surface areas, which varies according to land cover units. The larger areas are those of the
264 degraded vegetation and agricultural zone classes.

265 **Table 3. Image Area 2015**

Classes	Areas in Km ²	Percentages (%)
Water	6.33	1.36
Inhabited area and bare soil	10.52	2.26
Dense vegetation	43.40	9.32
Degraded vegetation	267.55	57.61
Agricultural area	104	22.39

266

267 ◆ The year 2025 shows a significant change in the classes of habitat/bare soil, agricultural area, and degraded vegetation,
 268 and a reduction in the classes of dense vegetation and water. Figure 6 presents the land cover map for the year 2025.



269

270 Figure 6: Land cover map for the year 2025

271 Table 4 shows the evolution of surface areas, which varies according to land cover units. Large areas are those of the
 272 classes degraded vegetation, agricultural zone, and bare soil.

273 **Table 4. Image Area 2025**

Classes	Areas in Km ²	Percentages (%)
Water	5.73	1.23
Inhabited area and bare soil	29.13	6.26
Dense vegetation	40.96	8.81
Degraded vegetation	272.72	58.68
Agricultural area	116.19	25.00

274

275

276 **3.3 Discussion**

The supervised classification method using the maximum likelihood algorithm was used to process Landsat TM 1985, ETM+ 2000, and OLI 2015 and 2025 images in this study. The confusion matrices of the supervised classifications yielded cartographic accuracies of 65%, 72%, 78%, and 87% for the 1985, 2000, 2015, and 2025 images, respectively. The resulting Kappa indices were 0.55, 0.63, 0.71, and 0.8 for the 1985, 2000, 2015, and 2025 images, respectively. According to Blum et al. (1995), index values corresponding to cartographic accuracy are considered to be very good agreement when the index is between 0.81 and 1. substantial agreement, when the index is between 0.61 and 0.80 and moderate agreement, when the index is between 0.41 and 0.60. The results for the year 2025 indicate an almost perfect agreement between cartographic accuracy and the truth on the ground (Chalifoux et al., 2006). Les coefficients de Kappa des années 2025 et 2015 sont supérieurs à ceux de 2000 et 1985. Cela s'explique logiquement par la proximité de la campagne de terrain, qui a eu lieu en 2025. Lorsque le coefficient de Kappa est compris entre 0,50 et 0,75, la classification adoptée est valable et les résultats peuvent être judicieusement utilisés (Pontius 2000). Consequently, the classifications used in this study are appropriate. Despite the cartographic details, there is some overlap between certain land-use classes. Three classes are the primary sources of confusion for these three classifications: dense forest, degraded forest, and cropland. This can be explained by the fact that the study area is located in a densely vegetated zone. It has been observed that in certain places, several cash crops, primarily coffee and cocoa, are grown under large trees. Similar observations apply to certain areas of degraded forest. From a distance, these areas appear as dense forests. However, up close, they are cultivated areas, cleared land, but covered by large trees. These classes behave similarly from a radiometric point of view and therefore have visually similar spectral responses (Obodai et al., 2019). This makes them difficult to differentiate in the satellite image and could therefore explain these confusions. The study of land cover and land use dynamics between 1985 and 2025 highlights a significant change in vegetation cover. This change is marked by a decline in the classes of dense vegetation, degraded vegetation, and agricultural land, to the detriment of the classes of water, bare soil, and habitats (see Figures 3, 4, 5, 6). The decline in vegetation and agricultural land is primarily due to mining activities (industrial and artisanal). Indeed, many gold miners illegally occupy forests and agricultural land. Furthermore, several hectares of forest have been destroyed to expand the activities of the Ity Mining Company (SMI). In fact, to expand its extraction operations, SMI bought several plantations (coffee, cacao, oil palm, etc.) from the local population. These factors have led to a significant decrease in plantation areas in the region. The reduction of forest areas due to gold mining activities has been reported by several authors in Peru. Martinez et al. (2018) noted a loss of approximately 50,000 hectares of forest between 1991 and 2016. Several studies conducted in Ghana on vegetation cover dynamics in mining areas have noted the loss of significant forest areas to gold mining sites. Donkor and Agyemang (2015) reported a massive loss of forest cover in the Ankora basin between 1990 and 2010, with a rate of decline of 40%, representing an estimated area of 200,000 m².

The tool we used to conduct this study is a powerful instrument, but its limitations in analyzing land-use dynamics primarily relate to data quality, the complexity of temporal analyses, and technical and hardware constraints. For better results, it is often recommended to combine QGIS with Google Earth Engine.

311

312 **4. CONCLUSION**

313

314 The study of land cover and land use dynamics revealed a significant change in the five classes (dense vegetation, degraded
315 vegetation, agricultural land, bare soil and habitats, and water). This change manifested as a decline in the dense vegetation
316 class, to the benefit of the bare soil and habitats, degraded vegetation, agricultural land, and water classes. Gold panning
317 and industrial gold mining are the main drivers of forest cover dynamics over the past forty years.

318 **ACKNOWLEDGEMENTS**

319

320 The authors also thank the prefecture of Zouan-Hounien for facilitating our field visits.

321

322 **COMPETING INTERESTS**

323

324 Authors have declared that no competing interests exist

325

326

327 **REFERENCES**

328

329 Aka, N. (2014) Impact des activités anthropiques sur les ressources en eau du département d'Abengourou (est de la Côte
330 d'Ivoire) : Apport de l'hydroclimatologie. De la télédétection et de l'hydrochimie. Thèse de Doctorat de l'Université Félix
331 Houphouët Boigny de Cocody, Abidjan, 270 p.

332
333 Amandine carine, n. M., youan ta, m., kamenan satti, j.-r., assoma, t. V., & jourda, j. P. (2023). Cartographie automatique
334 des zones inondées et evaluation des dommages dans le district d'abidjan à l'aide de l'imagerie satellitaire radar sentinel1
335 depuis google earth engine. European scientific journal, esj, 22, 124. Retrieved from
336 <https://eujournal.org/index.php/esj/article/view/17285>

337 AMEDEE (2017): <http://www.amedee-network.ma/index.php/ateliers-workshop#> atelier « mine et développement durable »
338 consulté le 10 Avril 2026.

339 ANDRÉASSIAN V., 2004. couvert forestier et comportement hydrologique des bassins versants. la houille blanche/N° 2,
340 31–35.

341 BLUM A., FELDMANN L., BRESTER F. et JOUANNY P. (1995). Intérêt du Calcul du Coefficient Kappa dans l'Evaluation
342 d'une Méthode d'Imagerie. Journal of Radiology, Vol.76, pp. 441 - 443.

343
344 Brou, L. A. (2019). Modélisation de la Dynamique Hydrologique du Fleuve Cavally sous l'Influence de fortes Pressions
345 Anthropiques dans la Zone de Zouan-Hounien (Côte d'Ivoire). Thèse de Doctorat, UFR Environnement, Daloa: Université
346 Jean Lorougnon Guédé, 272 p.

347
348 CHALIFOUX S., MIROSLAV N., CHARLES L., RASIM L. and RICHARD F. (2006). Cartographie de l'occupation et de
349 l'utilisation du sol par imagerie satellitaire landsat en hydrogéologie. Télédétection, Vol.6, N°1, pp. 9 - 17.

350
351 Derdjini H., (2017). Cartographie des changements de l'occupation du sol dans la plaine de la MITIDJA à partir des images
352 landsat. Mémoire de DEA, ENSH ARBAOUI Abdellah.

353
354 DGMG (DIRECTION GENERALE DES MINES et DE LA GEOLOGIE) (2013) : Fiche sectorielle Mines en bref, 2 p.

355
356 DONKOR P. and AGYEMANG F. (2015). Analysis of Spatial Planning Options: Ankobra, The USAID/Ghana Sustainable
357 Fisheries Management Project (SFMP). Narragansett, RI: Coastal Resources Center, Graduate School of Oceanography,
358 University of Rhode Island and Spatial Dimensions. GH2014_ACT046_SpS. 49 p.

359
360 Ettien, D. Z. (2005). étude d'évaluation de l'Impact des Exploitations Minières sur l'Environnement et les Populations en
361 Afrique Occidentale: Cas de la Mine d'or d'Ity dans la Région Semi-Montagneuse de l'Ouest de la Côte d'Ivoire. Contribution
362 of the Geographical Information System (GIS) and Remote Sensing. Thèse Unique de Doctorat, Abidjan: Université de
363 Cocody, 178 p.

364
365 FAO., 2018. Travaillons avec les divers secteurs pour arrêter la déforestation et étendre les superficies forestières- de
366 l'aspiration à l'action. Actes de Conférence internationale 20–22/02/2018, 37 p.

367
368 FAO., 2020. La situation des forêts du monde 2020. Forêts, Biodiversité et activité humaine. 32 p.

369
370 FAO., 2020. Global Forest Resources Assessment. The data in FRA 2020, 16p.

371
372 Feybesse, J. L., Milesi, J. P., Verhaeghe, PH., et Johan, V. (1990). Le domaine de Touleupley-Ity (Côte d'Ivoire) - une unité
373 « birimiène » charriée sur les gneiss archéens du domaine de Kénéma-Man lors des premiers stades de l'orogénèse
374 éburnéenne. Comptes Rendus de l'Académie des Sciences , Paris 310, II : 285- 291.

375
376 KOUASSI A. M., (2007). Caractérisation d'une modification éventuelle de la relation pluie-débit et ses impacts sur les
377 ressources en eau en Afrique de l'Ouest : cas du bassin versant du N'zi (Bandama) en Côte d'Ivoire. Thèse de Doctorat
378 unique, Université de Cocody, 210 p.

379
380 MARTINEZ G., MCCORD S. A., DRISCOLL C. T., TODOROVA S., WU S., ARAUJO J. F., and al., (2018). Mercury
381 Contamination in Riverine Sediments and Fish Associated with Artisanal and Small-Scale Gold Mining in Madre de Dios,
382 206 Peru. International Journal of Environmental Research and Public Health, Vol.15, N°8, pp. 1 - 15.

383
384 OBODAI J., ADJEI. K. A., ODAI S. N. and LUMOR M. (2019). Land use/land cover dynamics using landsat data in a gold
385 mining basin-the Ankobra, Ghana. Remote Sensing Applications: Society and Environment, Vol.13, pp. 247 - 256.

386
387 PAPON, A. (1973). Géologie et minéralisation du Sud-Ouest de la Côte d'Ivoire. Mem. Bur. Res. Géol. Paris, N° 80, 284 p.

386 PONTIUS J. R. G. (2000). Quantification error versus location error in comparison of categorial maps. *Photogrammetric*
387 *Engineering and remote sensing*, Vol.66, N°8, pp. 1011 1016.
388

389 SORO, B. (2011). Agriculture et matières premières en Côte d'Ivoire : Le cacao, le café, le coton, l'or, le sucre (...) en chute
390 libre / La crise financière internationale sévit, *Le Mandat*, <http://www.koffi.net/koffi/rechercheMultiple/a/43/Retirer>, consulté
391 le 02/09/2014
392

393 Séverin BIAOU, Felix HOUETO, Gérard GOUWAKINNOU, Samadori Sorotori Honoré BIAOU, Beranger AWESSOU et al.
394 Dynamique spatio-temporelle de l'occupation du sol de la forêt classée de Ouénou-Bénou au NordBénin. Conférence
395 OSFACO : Des images satellites pour la gestion durable des territoires en Afrique, Mar2019, Cotonou, Bénin. (hal-
396 02189367)

397 Tong, Q., Qiu, F., 2020. Population growth and land development: investigating the bi- directional interactions. *Ecol. Econ.*
398 169, 106505. <https://doi.org/10.1016/J.ECOLECON.2019.106505>.
399

400 Tricart J., Avenard J.-M., Eldin M., Girard G., Sircoulon J., Touchebeuf P., et al., (1973). Une monographie physique de la
401 Côte-d'Ivoire. In: *Annales de Géographie*, JSTOR, pp. 369–372.
402

403 Yao K.T. (2009). Hydrodynamisme dans les aquifères de socle cristallin et cristallophyllien du Sud-Ouest de la Côte d'Ivoire
404 : cas du département de Soubré : apports de la télédétection, de la géomorphologie et de l'hydrogéochimie. Océan,
405 Atmosphère. Conservatoire national des arts et metiers - CNAM; Université de Cocody - Côte d'Ivoire, 2009.